




Article

Characterization and Structural Determination of Cold-Adapted Monodehydroascorbate Reductase, MDHAR, from the Antarctic Hairgrass *Deschampsia Antarctica*

Ae Kyung Park ^{1,2,†}, Il-Sup Kim ^{3,†} , Hackwon Do ^{1,4} , Hyun Kim ¹, Woong Choi ¹, Seung-Woo Jo ⁵, Seung Chul Shin ¹, Jun Hyuck Lee ^{1,6}, Ho-Sung Yoon ^{3,5,7} and Han-Woo Kim ^{1,6,*} 

¹ Unit of Research for Practical Application, Korea Polar Research Institute, Incheon 21990, Korea; parkak1003@korea.kr (A.K.P.); hdo@houstonmethodist.org (H.D.); kh@kopri.re.kr (H.K.); woong@kopri.re.kr (W.C.); ssc@kopri.re.kr (S.C.S.); junhyucklee@kopri.re.kr (J.H.L.)

² Division of Bacterial Diseases, Center for Laboratory Control of Infectious Diseases, Korea Centers for Diseases Control and Prevention, Chungcheongbuk-do 28159, Korea

³ Advanced Bioresource Research Center, Kyungpook National University, Daegu 41566, Korea; 92kis@hanmail.net (I.-S.K.); hsy@knu.ac.kr (H.-S.Y.)

⁴ Department of Pathology and Genomic Medicine, Houston Methodist Hospital Research Institute, Houston, TX 77030, USA

⁵ Department of Energy Science, Kyungpook National University, Daegu 41566, Korea; jsw8796@gmail.com

⁶ Department of Polar Sciences, University of Science and Technology, Incheon 21990, Korea

⁷ School of Life Sciences, BK21 Plus KNU Creative BioResearch Group, Kyungpook National University, Daegu 41566, Korea

* Correspondence: hwkim@kopri.re.kr; Tel.: +82-32-760-5526

† These authors contributed equally to this work.

Received: 18 September 2019; Accepted: 17 October 2019; Published: 18 October 2019



Abstract: Ascorbic acid (AsA) is an abundant component of plants and acts as a strong and active antioxidant. In order to maintain the antioxidative capacity of AsA, the rapid regeneration of AsA is regulated by dehydroascorbate reductase (DHAR) and monodehydroascorbate reductase (MDHAR). To understand how MDHAR functions under extreme temperature conditions, this study characterized its biochemical properties and determined the crystal structure of MDHAR from the Antarctic hairgrass *Deschampsia antarctica* (DaMDHAR) at 2.2 Å resolution. This allowed for a structural comparison with the mesophilic MDHAR from *Oryza sativa* L. *japonica* (OsMDHAR). In the functional analysis, yeast cells expressing DaMDHAR were tolerant to freezing and thawing cycles. It is possible that the expression of DaMDHAR in yeast enhanced the tolerance for ROS-induced abiotic stress.

Keywords: monodehydroascorbate reductase; Antarctic hairgrass; cold adaptation

1. Introduction

There are only two species of flowering plants in the Antarctic Peninsula, Antarctic hair grass (*Deschampsia antarctica*) and Antarctic pearlwort (*Colobanthus quitensis*). During their entire life cycles, Antarctic plants are exposed to multiple abiotic stresses, including extreme temperatures, varying oxygen concentrations, drought, nutrient depletion, very short growing seasons, common summer frosts, strong winds, low light quality, and photoperiod changes [1,2]. Low temperatures, particularly freezing temperatures, can dramatically impact plants at cellular to ecosystem scales [3]. To cope with

cold stress, plant species have evolved adaptations in physiological and molecular functions to boost their cold tolerance by increasing their metabolic rates upon cold acclimation [4,5]. For example, plants in the Antarctic region have long life cycles, an extended primordium development of leaves and flowers, well-developed root systems, and efficient photosynthetic and respiratory systems at 10 °C or lower [1,6,7].

Various cellular changes that are induced by low temperatures lead to the excess accumulation of toxic compounds, especially reactive oxygen species (ROS) [8]. The end result of ROS accumulation is oxidative stress [9]. Reactive oxygen species can induce DNA damage, protein oxidation, membrane lipid peroxidation, and the destruction of pigments [10]. Therefore, a considerable amount of research has been conducted to explore the correlation between ROS scavenging and plant stress tolerance under extreme temperatures, given that climate change due to global warming is causing enormous harm to annual crop production. As such, the development of useful plant genetic resources that confer enhanced resistance to environmental stress is becoming increasingly important, and interest in this field is growing [11].

To increase their probability of survival, plants have developed two efficient forms of antioxidant machinery [12]. The first group is comprised of enzymatic components, including superoxide dismutase and catalase. The second group is formed by non-enzymatic antioxidants, including ascorbic acid (AsA) and glutathione (GSH). Among them, AsA is an abundant plant component and acts as a strong and active antioxidant [13]. In order to maintain the antioxidative capacity of AsA, the rapid regeneration of AsA is regulated by dehydroascorbate reductase (DHAR) and monodehydroascorbate reductase (MDHAR) in the AsA-GSH cycle [14–16]. There have been several reports that the overexpression of either of DHAR or MDHAR results in enhanced plant tolerance to various stressors [17–20]. In particular, it has been suggested that the role of MDHAR in the AsA regeneration cycle is more efficient than that of DHAR under conditions of strong oxidative stress [21]. Therefore, this conclusion indicates that an improvement in temperature stress tolerance in plants is often related to the enhanced activity of enzymes involved in antioxidant systems [11].

Deschampsia antarctica and *C. quitensis* are very useful resources for research on responses to stress due to a changing environment as these are the only flowering plants that have been able to adapt to the extreme environment of Antarctica. As these polar plants have adaptations to help them survive their harsh environment, it is possible to use them as models for research into the mechanisms by which plants respond and adapt to the environment.

Deschampsia antarctica is a perennial plant that belongs to the Poaceae family. As various basic experimental methods have been relatively well developed for its use in research compared to *C. quitensis*, it is likely to become a model plant in the field of polar plant research as well as a genetic resource for understanding stress resistance [22,23]. A genomic analysis of *D. antarctica* indicates that it also carries MDHAR-like genes (*DaMDHAR*). However, little is known about the mechanisms of stress adaptation in Antarctic plants. Therefore, a description of the molecular properties of the *DaMDHAR* involved in adaptations in Antarctic plants is of fundamental scientific importance and is valuable to understand how plant metabolisms adapt under extreme conditions.

In the present study, *Saccharomyces cerevisiae* and *Escherichia coli* strains into which *DaMDHAR* gene were fabricated to better understand the mechanisms by which *D. antarctica* responds to environmental stresses and to characterize its value as a genetic bio-resource. A cDNA encoding *DaMDHAR* was cloned and its function was analyzed in *S. cerevisiae* as a eukaryotic unicellular microorganism, that is widely distributed in natural environments and in association with various insects, animals, and plants. Furthermore, this study expressed and purified the *DaMDHAR* protein for a more detailed characterization and determined the crystal structure of *DaMDHAR* at 2.2 Å resolution. This allows for a structural comparison with the previously reported MDHAR of *Oryza sativa* L. *japonica* (*OsMDHAR*) [21]. Furthermore, these findings improve the understanding of the development of low temperature-tolerant yeast strains and suggest a survival strategy for Antarctic plants exposed to extreme environments.

2. Materials and Methods

2.1. Cloning and Protein Expression of DaMDHAR in Escherichia Coli

The total RNA was isolated from the leaves of *D. antarctica* plants using the RNeasy Plant Mini kit (Qiagen, Hilden, Germany), and the cDNA was synthesized by a reverse transcription-polymerase chain reaction (RT-PCR). The *DaMDHAR* coding region was amplified from the cDNA by PCR using Pfu polymerases (Roche, Basel, Switzerland) with forward (5'-CGATAAGAATTCATGGCGACGGAGAAGCACTTC-3') and reverse (5'-CGATAACTCGAGTCAGATCTTGCTGGCGAACAGG-3') primers. The reaction conditions were as follows: The initial denaturation was at 94 °C for 3 min, followed by 30 cycles at 94 °C for 30 s, 58 °C for 30 s, 72 °C for 1.5 min, and a final extension at 72 °C for 7 min. The amplified PCR products were ligated into the pET-28a(+) vector after digestion with EcoRI and XhoI restriction enzymes (Enzynomics, Daejeon, South Korea), which contain a thrombin cleavable N-terminal hexa-histidine tag (Figure S1, Supplementary Materials). Then, the recombinant plasmid was transformed into the *E. coli* strain BL21(DE3) for protein expression. The cells were grown at 37 °C (310 K) in Luria-Bertani (LB) medium containing 50 µg mL⁻¹ kanamycin (Sigma-Aldrich, St. Louis, MO, USA). When the OD₆₀₀ reached 0.6, the protein expression was induced using 0.2 mM isopropyl β-D-L-thiogalactopyranoside (IPTG) (Sigma-Aldrich, St. Louis, MO, USA). The cells were harvested after a 20 h induction at 25 °C (298 K). The pelleted cells were resuspended using buffer A (50 mM sodium phosphate (Sigma-Aldrich, St. Louis, MO, USA), 300 mM NaCl (Sigma-Aldrich, St. Louis, MO, USA), and 5 mM imidazole (Sigma-Aldrich, St. Louis, MO, USA) at pH 8.0 supplemented with 0.2 mg mL⁻¹ lysozyme (Sigma-Aldrich, St. Louis, MO, USA) and 0.5 mM fluoride PMSF and lysed by sonication. The lysate was centrifuged and loaded onto a gravity-flow Ni-NTA column which was equilibrated with buffer A. The column was washed with 20 column volumes of buffer B (50 mM sodium phosphate, 300 mM NaCl, and 20 mM imidazole at pH 8.0) and then eluted with a 2-bed volume of buffer C (50 mM sodium phosphate, 300 mM NaCl, and 300 mM imidazole at pH 8.0). To remove the N-terminal his-tag, thrombin (5 NIH units) was added to the eluted protein solution and the mixture was incubated for 24 h at 4 °C. The protein was purified to its final state by gel filtration on a HiLoad 16/60 Superdex 200 column (GE Healthcare, Little Chalfont, UK) that was previously equilibrated with 20 mM Tris-Cl (Sigma-Aldrich, St. Louis, MO, USA) and 150 mM NaCl at pH 8.0. The final protein concentration was 20 mg mL⁻¹.

2.2. Enzymatic Activity

The activity of MDHAR was assayed spectrophotometrically. The assay was performed at 25 °C with a reaction mixture containing 50 mM potassium phosphate, 0.2 mM NADH, 2 mM AsA, and 1 unit of AsA oxidase at pH 7.2 (Sigma-AldrichTM, Merck, St. Louis, MO, USA). The activity of MDHAR was measured by monitoring the decrease in absorbance at 340 nm resulting from NADH oxidation. The activity was calculated using an absorbance coefficient of 6.2 mM⁻¹ cm⁻¹ [18].

2.3. Crystallization and Structure Refinement

The initial crystallization conditions of DaMDHAR were screened in MRC 96-well crystallization plates using commercially available screening kits with the mosquito crystallization robot (TTP Labtech, UK). A total of 0.2 µL protein solution (19.5 mg mL⁻¹) was mixed with the same volume of reservoir solution and equilibrated against an 80-µL reservoir solution at 25 °C (298 K). The initial crystals were obtained under the following conditions: 0.1 M Tris-HCl, 0.2 M calcium chloride, and 25% (w/v) PEG 4000 at pH 8.5. Then, the crystal condition optimization was performed by scaling up the hanging-drop vapor-diffusion method using 24-well plates. The crystals were flash-frozen without a cryoprotectant in a stream of liquid nitrogen (100 K) for data collection. The X-ray diffraction data were collected with a 2.2 Å resolution at the beamline BL-5C of the Pohang Accelerator Laboratory (Pohang, Korea). All data sets were indexed, processed, and scaled using the HKL2000 software package [24]. The statistics for data collection are summarized in Table 1. The crystal structure of DaMDHAR was determined by the

molecular replacement (MR) method, using the MOLREP program and the CCP4 package [25] with MDHAR of *O. sativa* L. *japonica* (PDB ID: 5JCI, sequence identities 90%) as a reference [21]. Then, the refinement was performed using Refmac5 [26] and the model was rebuilt with the COOT program [27]. The stereochemical qualities of all final models were assessed with MolProbity and were excellent [28]. The refinement statistics are also summarized in Table 1. All structural figures were generated using the PyMOL program [29].

Table 1. X-ray diffraction data collection and refinement statistics.

Data Set	DaMDHAR
X-ray source	PAL-5C beam line
Space group	$P2_1 2_1 2_1$
cell axes (Å)	74.15, 88.85, 129.35
cell angles (deg)	90, 90, 90
Wavelength (Å)	0.9796
Resolution (Å)	28.12–2.20 (2.36–2.32)
Total reflections	69131
Unique reflections	19691 (911)
Average I/ σ (I)	42.7 (22.4)
R_{merge}^a	0.067 (0.165)
Redundancy	3.5 (3.5)
Completeness (%)	97.0 (90.2)
Refinement	
Resolution range (Å)	33.81–2.32 (2.38–2.32)
No. of reflections of working set	18706 (1341)
No. of reflections of test set	964 (47)
No. of amino acid residues	554
No. of water molecules	208
R_{cryst}^b	0.176 (0.165)
R_{free}^c	0.235 (0.239)
R.m.s. bond length (Å)	0.0096
R.m.s. bond length (°)	1.596
Average B value (Å ²) (protein)	27.9
Average B value (Å ²) (solvent)	31.0

^a $R_{\text{merge}} = \sum |I - \langle I \rangle| / \sum I$. ^b $R_{\text{cryst}} = \sum ||F_o| - |F_c|| / \sum |F_o|$. ^c R_{free} calculated with 5% of all reflections excluded from the refinement stages using high-resolution data. Values in parentheses refer to the highest resolution shells.

2.4. Protein Data Bank Accession Number

The coordinates of the structure together with its structure factor have been deposited in the Protein Data Bank (<http://www.rcsb.org/pdb>) with the accession code 6KRT.

2.5. Establishment of DaMDHAR-Expressing Yeast

The sense (GPD-F) and antisense (GPD-R) primer set used for the PCR cloning of the DaMDHAR gene (GenBank accession number: MN442319) is as follows: 5'-ATTCTAGAACTAGTGGATCCATGGCGACGGAGAAGCACTTC-3' and 5'-TCGACGGTATCGATAAGCTTTCAGATCTTGCTGGCGAACAGG-3'. The nucleotide sequences of the p426GPD vector corresponding to BamHI and HindIII are underlined. The PCR amplicon and yeast expression vector p426GPD digested with the endonucleolytic enzymes BamHI and HindIII were purified using PCR SV MINI (GeneAll, Seoul, Korea). Then, the purified PCR product was cloned into p426GPD under the control of a glyceraldehyde-3-phosphate dehydrogenase (GPD) promoter (Euroscarf, Frankfurt, Germany) via a sequence- and ligation-independent cloning method with T4 DNA polymerase [30]. After the sequence confirmation, the p426GPD::DaMDHAR construct (shown in Figure S1A) was transformed into *S. cerevisiae* BY4741 cells using the PEG/LiCl method [31]. The transformants were selected by plating cells on SD agar medium (0.67% yeast nitrogen base

without amino acids, ammonium sulfate 0.192% yeast synthetic drop-out medium lacking uracil, 2% glucose, and 2% bacto agar) at 28 °C for 3 days. A single colony was streaked, cultured under the same conditions, and used for subsequent experiments. The genotypes of the yeast strains used in this study are shown in Table S1.

2.6. Stress Tolerance Assay

The yeast cells (initial concentration adjusted to 1×10^6 cells mL⁻¹) were grown overnight at 28 °C and inoculated into YPD broth medium (1% yeast extract, 2% peptone, and 2% dextrose) and cultured for 6 h with shaking (160 rpm). The mid-log phase yeast cells (OD₆₀₀ \approx 0.5) were then challenged with freezing and thawing (FT) conditions. To induce FT stress, the cells were frozen at −80 °C for 0.5 h and thawed at 25 °C for 1 h. This step was repeated 6 times. Afterwards, the stressed yeast cells were serially diluted 10-fold (100 to 10⁻⁴). A 5-μL aliquot of each dilution was spotted onto YPD agar plates (YPD plus 1.5% agar), incubated for 2–3 days at 28 °C, and photographed.

2.7. Western Blot Analysis

The yeast cells that reached a mid-log phase were harvested by centrifugation at 2000× *g* for 3 min at 4 °C. The crude protein extracts were prepared using glass beads. The cells were washed three times with cold phosphate-buffered saline (PBS; Invitrogen™) and resuspended in lysis buffer containing 50 mM HEPES, 5% glycerol, 10 mM 1,4-dithiothreitol (DTT), 1 mM phenylmethylsulfonyl fluoride (PMSF), and protease inhibitor cocktail (Sigma-Aldrich™) at pH 7.2 with an equal volume of glass beads (425–600 microns; Sigma-Aldrich™). After vigorously vortexing for 1 min on ice four times at 2-min intervals, the lysates were centrifuged at 13,000× *g* for 20 min at 4 °C, and the supernatants were used as protein extracts. The protein concentration was determined using Protein Dye Reagent (Bio-Rad, Hercules, CA, USA). The total protein (20 μg) was resolved by SDS-PAGE and electrophoretically transferred to a PVDF membrane. The membrane was blocked with 5% non-fat skim milk in Tris/HCl-buffered saline containing 0.05% Tween 20 (TBST) and 0.02% sodium azide and then incubated at 4 °C overnight with an anti-OsMDHAR antibody appropriately diluted in TBST. The blot was washed four times for 40 min with TBST and then incubated for 90 min at 25 °C with appropriately diluted goat anti-rabbit IgG-HRP secondary antibody (Santa Cruz Biotechnology Inc., Dallas, TX, USA). After washing four times for 40 min with TBST, the bands were visualized using the ECL Western Blotting Detection Reagent (GE Healthcare). The anti-tubulin (Tub) antibody was used as a loading control (Santa Cruz Biotechnology Inc.). The anti-OsMDHAR antibody was produced in rabbits inoculated with purified OsMDHAR protein. Other primary antibodies were used as previously reported [1].

2.8. Statistical Analysis

The significant differences in the measured parameters were identified using Origin Pro 8.0. All experiments were independently performed at least three times. The results are expressed as the mean ± standard deviation (SD). The results of the spotting assays are representative of at least two independent experiments performed under identical conditions.

3. Results

3.1. Enzymatic Properties of DaMDHAR

To examine the catalytic properties of DaMDHAR, the recombinant enzyme was purified. To determine the optimal pH and temperature for DaMDHAR, the enzymatic activity was assayed at different pH levels and temperatures. This study found that the pH optimum for DaMDHAR was alkaline. The enzyme was stable at pH 7.5 to 9.5, retaining more than 80% of its activity in this pH range. It was found that the optimal pH was 8.5 (as shown in Figure 1A) and the activity of DaMDHAR

increased with increasing pH up to pH 8.5. At pH 8.5, the enzymatic activity began to decline and at pH 10.5, the relative enzymatic activity was only approximately 20%.

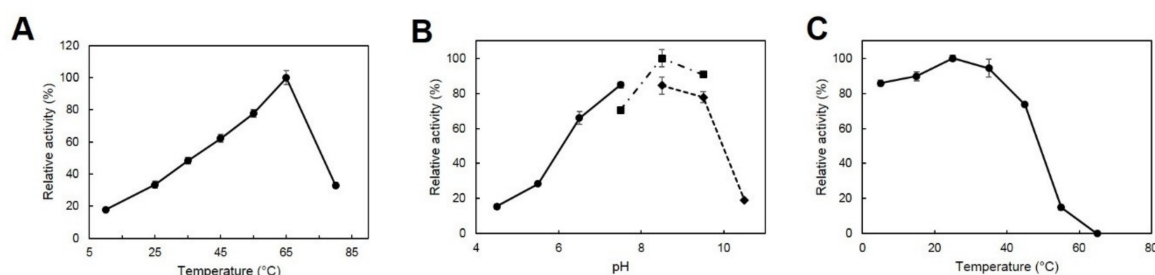


Figure 1. Effects of temperature and pH on the enzyme activity of DaMDHAR. (a) Enzyme activity was measured at various temperatures as described in the Materials and Methods section. The activity value shown at 65 °C was taken as 100%. (b) The effect of pH was studied with a sodium acetate buffer (pH 3.5 to 7.5, closed circle), Tris-Cl buffer (pH 7.5 to 9.5, closed square), and glycine buffer (pH 8.5 to 10.5, closed diamond). (c) The thermal stability of DaMDHAR was studied by pre-incubating DaMDHAR at various temperatures for 30 min. After the 30 min pre-incubation, the residual activity of DaMDHAR was calculated by taking the non-heated DaMDHAR activity as 100%.

The effects of temperature on the activity and stability of DaMDHAR were also determined. The optimum temperature for DaMDHAR activity was 65 °C (Figure 1B). However, even at 10 °C, it displayed approximately 20% of its maximum activity, and half of its activity was lost at temperatures over 75 °C. Furthermore, DaMDHAR showed broad temperature optima that ranged from 35 °C to 75 °C in which it retained more than 50% of its activity. However, meaningful data in the 0 to 5 °C temperature range could not be obtained. The thermal stability of DaMDHAR was measured by incubating the enzyme at different temperatures for 30 min and then assaying the residual activity under optimal pH at room temperature (Figure 1C). It was found that DaMDHAR was stable from 5 °C to 35 °C and it retained more than 80% of its initial activity in this temperature range. Even at 5 °C for 30 min, its activity was retained by more than 80%. However, the residual activity of the enzyme was less than 20% when incubated at 55 °C. Therefore, this indicates that DaMDHAR displays an apparent thermal stability that is shifted toward low temperatures as well as heat lability.

3.2. Crystal Structure of DaMDHAR

The structure of DaMDHAR was determined by a molecular replacement (MR) method at 2.2 Å, and two molecules were found in the asymmetric unit. The overall structure of DaMDHAR indicates that it consists of three domains: an NAD(P)-binding domain, an FAD-binding domain, and a C-terminal domain (Figure 2). This is consistent with the structure of OsMDHAR [21]. The MDHAR proteins share structural similarity with those of iron-sulphur protein reductases, except for a unique long loop of 63–80 residues that cover the active site. A previous report regarding the structure of OsMDHAR revealed that the conserved tyrosine residue mediates electron transfer from NAD(P)H to bound substrates via FAD [21]. The bound FAD molecule imparts a yellow color to the OsMDHAR crystals. Likewise, the DaMDHAR crystals retained their yellow color, implying that DaMDHAR also contains a FAD molecule (Figure 2A).

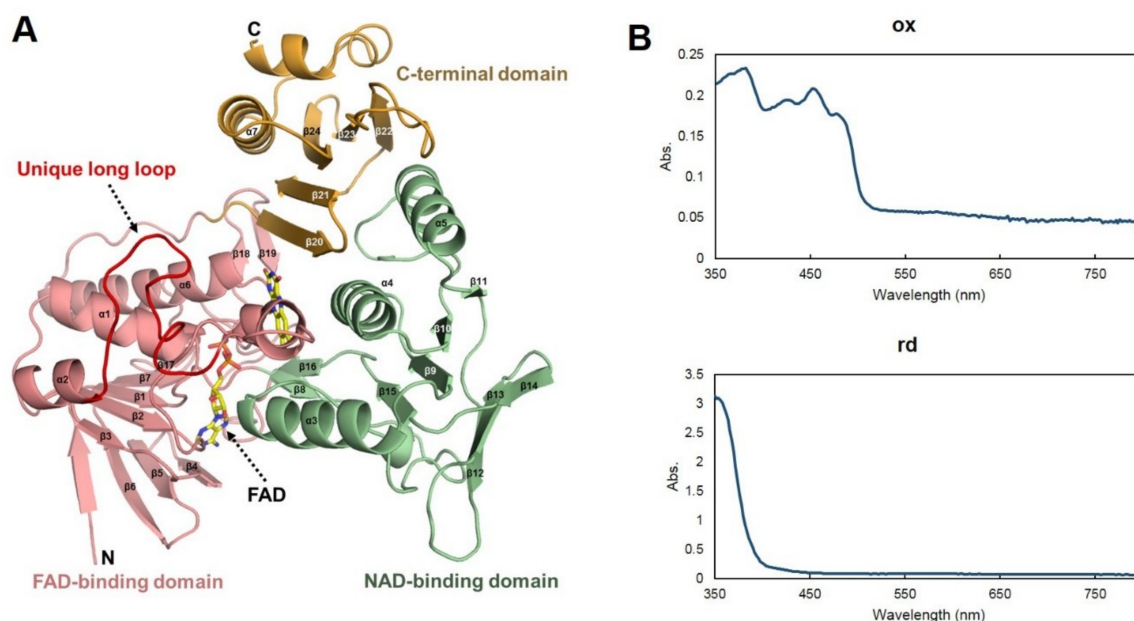


Figure 2. Overall structure (A) and UV-visible spectrum (B) of DaMDHAR. The FAD, NAD-binding domains, and C-terminal domains are colored light pink, light green, and yellow, respectively. Specifically, the bound FAD molecule is presented as a stick model. The UV-visible spectrum of OsMDHAR was monitored in the absence (oxidized, ox) and the presence of NADH (reduced, rd) in the solution state.

Previous reports have shown that NAD binding led to a butterfly-like movement of the isoalloxazine ring of FAD, which quenched the intrinsic yellow color of FAD [21,32]. In the case of DaMDHAR, the yellow color became transparent upon the addition of NADH. The butterfly-like movement of FAD was indirectly measured by observing the UV-visible spectrum in the absence (oxidized, ox) and presence of NADH (reduced, rd; Figure 2B).

The multiple sequence alignments indicated that the participating residues of NAD(P), FAD, and the substrate were well conserved in DaMDHAR. Therefore, the electron transfer mechanism of DaMDHAR was suggested to proceed as has been observed in OsMDHAR (Figure 3A). The Tyr349 of DaMDHAR would thus mediate the electron transfer via FAD from NADH, which is a preferred electron donor to AsA, and Arg320 might play an important role in the interactions with the bound substrate. Although the two MDHAR proteins, DaMDHAR and OsMDHAR, originated from mesophilic and Antarctic plants, respectively, they share approximately 90% of their sequence identities. Therefore, there are approximately 40 residue differences only between these two proteins. When the aforementioned 40 residues were marked in the structure of DaMDHAR, it was noticed that almost all of the residues were located on the surface of the protein (Figure 3B). Among the 40 residues, there were no conserved residues that contributed to NAD(P) and substrate binding. On the other hand, two residues, Arg40 and Ser319, interacted with FAD. As shown in Figure 3C, Lys40 and Ala319 of OsMDHAR were replaced by Arg40 and Ser319 in DaMDHAR, respectively.

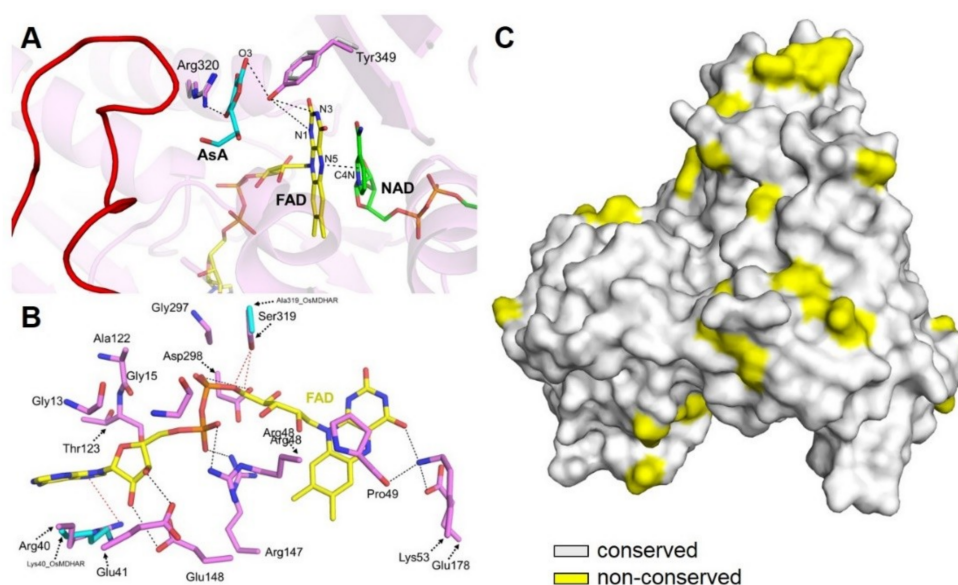


Figure 3. Structural comparison of DaMDHAR and OsMDHAR. (A) Close-up view of the electron transfer pathway from NAD to ascorbic acid (AsA) via FAD by the flanking Tyr349 on the superimposed structure of both proteins. (B) Close-up view of the FAD binding site. The residues that participate in hydrogen bonding and van der Waals interactions are shown as stick models and are colored green and blue, respectively. The bound FAD is colored yellow. (C) The superimposed structure of DaMDHAR and OsMDHAR showed that the amino acids on the surface of both proteins were highly variable.

3.3. Stress Response in DaMDHAR-Expressing Yeast

The *in vitro* assays showed that the purified DaMDAHR protein was very stable at low temperatures (4–37 °C) when compared to high temperatures (above 40 °C; Figure 1C). This suggests that chill-friendly DaMDHAR developed as an evolutionary mechanism for *D. Antarctica* to survive and grow under extreme environmental conditions. Based on these results, this study investigated whether *DaMDHAR* could improve an acquired tolerance to abiotic stress in *S. cerevisiae* under low temperature conditions.

A cDNA containing the open reading frame (ORF) of *DaMDHAR* was subcloned into the yeast expression vector p426GPD, which allows for the constitutive expression of a target gene under the control of the GPD yeast promoter (Figure S1A). To check whether the *DaMDHAR* gene was expressed at a translational level in yeast, an immunoblotting assay was performed. As shown in Figure 4A, an immunoblotting analysis using an antibody against OsMDHAR detected a single band at approximately 45 kDa that was derived from DaMDHAR in the crude extract prepared from DM and DA cells, but not in the extract prepared from WT and A2 cells. To determine the relationship between the heterologous *DaMDHAR* expression and stress tolerance in yeast, a cell survival assay was performed. The spotting assay demonstrated that *DaMDHAR*-expressing DM cells increased their intrinsic stress tolerance when they were exposed to FT stress when compared to WT cells (Figure 4B). These phenotypic differences were strongly visualized when the FT stress cycle was repeated six times. There was no difference in either A2 or DA cells under FT stress (Figure 4C). The D-erythroascorbate (EAA) biosynthesis-related gene, *ARA2*, was deleted in A2 cells.

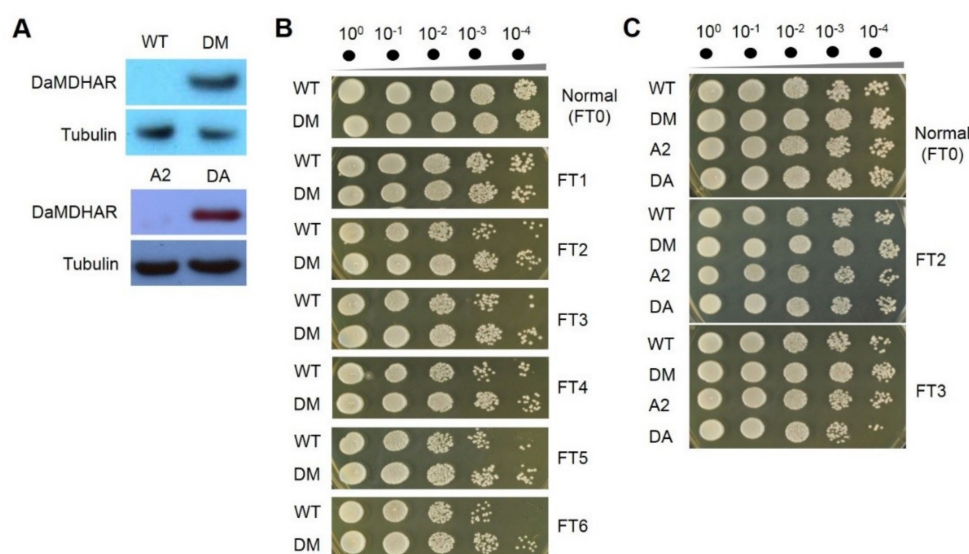


Figure 4. Stress response of *DaMDHAR*-expressing yeast during freezing and thawing (FT) cycles. (A) The *DaMDHAR* gene was subcloned to generate the p426GPD::*DaMDHAR* construct with *DaMDHAR* under the control of the constitutive *GPD* promoter. An immunoblotting assay was performed to examine whether *DaMDHAR* is expressed in this yeast strain. Tubulin (Tub) was used as a loading control. The molecular weight of the detected band was approximately 45 kDa. (B) Stress response to FT cycles was evaluated with a spotting assay. (C) Substrate specificity analysis of D-erythroascorbate for *DaMDHAR* was performed using BY4741 cells (*ara2Δ*) deficient for the *ara2* gene. The *ara2Δ* cells expressing *DaMDHAR* showed increased sensitivity to stress during FT cycles when compared to the DM cells even though there was no difference between the cells, including WT, A2, and DA. WT (BY4741 cells with p426GPD alone), DM (BY4741 cells harboring p426GPD::*DaMDHAR*), A2 (BY4741 cells (*ara2Δ*) deficient for the *ara2* gene), DA (*ara2Δ* cells harboring p426GPD::*DaMDHAR*). Tenfold dilutions (10^0 correspond to 1×10^6 cells) were spotted on the medium and incubated for 48 h.

4. Discussion

MDHAR is a critical enzyme involved in recycling oxidized ascorbate to reduced ascorbate in living organisms, such as plants, and is involved in growth, development, and stress responses. High temperatures affect a broad spectrum of cellular and metabolic components, including the AsA-GSH cycle in plants. However, the detailed roles of MDHAR involved in cold stress resistance remain unclear. Furthermore, no previous studies have established a relationship between MDHAR expression and the stress response in yeast, even though its function in plants and some microalgae has been well documented. For example, the overexpression of tomato MDHAR, *Arabidopsis thaliana* MDHAR (*AtMDHAR1*), and *OsMDHAR4* in transgenic plants is associated with an acquired tolerance for abiotic stressors, such as high and low temperatures, ozone, salt, polyethylene glycol, and radiation due to the improvement of redox homeostasis and photosynthesis through the co-activation of cell rescue enzymes [18,33,34]. The homologous MDHAR1 expression of *Chlamydomonas reinhardtii* increased cell viability by preventing lipid peroxidation given an elevated ascorbate pool under high light-induced oxidative stress, while the downregulation of the gene was associated with a decrease in cell survival due to increased hydrogen peroxide accumulation [35,36].

In conclusion, the high expression of *DaMDHAR* in a yeast strain increased its acquired tolerance for abiotic stress, specifically stress generated by freezing and thawing. It is possible that the expression of *DaMDHAR* in yeast enhanced the tolerance for ROS-induced abiotic stress and that various defense mechanisms acted synergistically by protecting the cells at different levels and generating rapid and effective defense responses under conditions of freezing and thawing stress.

Supplementary Materials: The following are available online at <http://www.mdpi.com/2073-4352/9/10/537/s1>, Figure S1: Schematic diagram of expression vector constructs for *Saccharomyces cerevisiae* and *Escherichia coli*, Table S1: Genotype of the strains used in this study.

Author Contributions: H.-W.K. conceived, supervised and organized the research activities. H.-W.K., A.K.P., and I.-S.K. wrote the manuscript with input from all the authors. A.K.P. and I.-S.K. performed biochemical properties experiments. A.K.P. and H.D. solved the crystal structure. H.K., W.C., and S.-W.J. contributed to sample preparation. S.C.S., J.H.L., and H.-S.Y. contributed to the interpretation of the results. All authors provided critical feedback and helped shape the research, analysis and manuscript.

Funding: This research was supported by a National Research Foundation of Korea Grant from the Korean Government (MSIT; the Ministry of Science and ICT) (NRF-2017M1A5A1013568) (KOPRI-PN19082) (Title: application study on the Arctic cold-active enzyme degrading organic carbon compounds), the Korea Polar Research Institute (KOPRI-PE19080) and a grant from the Next-Generation BioGreen 21 Program (No. PJ013240), Rural Development Administration, Korea.

Acknowledgments: We thank the staff at beamline BL-5C of the Pohang Accelerator Laboratory (Pohang, Korea).

Conflicts of Interest: The authors declare no conflicts of interest.

References

- Kim, I.S.; Kim, H.Y.; Kim, Y.S.; Choi, H.G.; Kang, S.H.; Yoon, H.S. Expression of dehydrin gene from Arctic *Cerastium arcticum* increases abiotic stress tolerance and enhances the fermentation capacity of a genetically engineered *Saccharomyces cerevisiae* laboratory strain. *Appl. Microbiol. Biotechnol.* **2013**, *97*, 8997–9009. [CrossRef] [PubMed]
- Bokhorst, S.; Bjerke, J.W.; Davey, M.P.; Taulavuori, K.; Taulavuori, E.; Laine, K.; Callaghan, T.V.; Phoenix, G.K. Impacts of extreme winter warming events on plant physiology in a sub-Arctic heath community. *Physiol. Plant.* **2010**, *140*, 128–140. [CrossRef] [PubMed]
- Loik, M.E.; Still, C.J.; Huxman, T.E.; Harte, J. In situ photosynthetic freezing tolerance for plants exposed to a global warming manipulation in the Rocky Mountains, Colorado, USA. *New Phytol.* **2004**, *162*, 331–341. [CrossRef]
- Theocharis, A.; Clement, C.; Barka, E.A. Physiological and molecular changes in plants grown at low temperatures. *Planta* **2012**, *235*, 1091–1105. [CrossRef] [PubMed]
- Isobe, K.; Takahashi, A.; Tamura, K. Cold tolerance and metabolic rate increased by cold acclimation in *Drosophila albomicans* from natural populations. *Genes Genet. Syst.* **2013**, *88*, 289–300. [CrossRef]
- Archambault, A.; Stromvik, M.V. PR-10, defensin and cold dehydrin genes are among those over expressed in *Oxytropis* (Fabaceae) species adapted to the arctic. *Funct. Integr. Genom.* **2011**, *11*, 497–505. [CrossRef]
- Chew, O.; Lelean, S.; John, U.P.; Spangenberg, G.C. Cold acclimation induces rapid and dynamic changes in freeze tolerance mechanisms in the cryophile *Deschampsia antarctica* E. Desv. *Plant Cell Environ.* **2012**, *35*, 829–837. [CrossRef]
- Mittler, R. Oxidative stress, antioxidants and stress tolerance. *Trends Plant Sci.* **2002**, *7*, 405–410. [CrossRef]
- Yin, H.; Chen, Q.M.; Yi, M.F. Effects of short-term heat stress on oxidative damage and responses of antioxidant system in *Lilium longiflorum*. *Plant Growth Regul.* **2008**, *54*, 45–54. [CrossRef]
- Awasthi, R.; Bhandari, K.; Nayyar, H. Temperature stress and redox homeostasis in agricultural crops. *Front. Environ. Sci.* **2015**, *3*, 11. [CrossRef]
- Suzuki, N.; Mittler, R. Reactive oxygen species and temperature stresses: A delicate balance between signaling and destruction. *Physiol. Plant.* **2006**, *126*, 45–51. [CrossRef]
- Sofo, A.; Scopa, A.; Nuzzaci, M.; Vitti, A. Ascorbate Peroxidase and Catalase Activities and Their Genetic Regulation in Plants Subjected to Drought and Salinity Stresses. *Int. J. Mol. Sci.* **2015**, *16*, 13561–13578. [CrossRef] [PubMed]
- Smirnoff, N. The function and metabolism of ascorbic acid in plants. *Ann. Bot.* **1996**, *78*, 661–669. [CrossRef]
- Asada, K. The water-water cycle in chloroplasts: Scavenging of active oxygens and dissipation of excess photons. *Annu. Rev. Plant Biol.* **1999**, *50*, 601–639. [CrossRef]
- Hossain, M.A.; Nakano, Y.; Asada, K. Monodehydroascorbate Reductase in Spinach-Chloroplasts and Its Participation in Regeneration of Ascorbate for Scavenging Hydrogen-Peroxide. *Plant Cell Physiol.* **1984**, *25*, 385–395.

16. Noctor, G.; Foyer, C.H. Ascorbate and glutathione: Keeping active oxygen under control. *Annu. Rev. Plant Biol.* **1998**, *49*, 249–279. [\[CrossRef\]](#)
17. Eltayeb, A.E.; Kawano, N.; Badawi, G.H.; Kaminaka, H.; Sanekata, T.; Morishima, I.; Shibahara, T.; Inanaga, S.; Tanaka, K. Enhanced tolerance to ozone and drought stresses in transgenic tobacco overexpressing dehydroascorbate reductase in cytosol. *Physiol. Plant.* **2006**, *127*, 57–65. [\[CrossRef\]](#)
18. Eltayeb, A.E.; Kawano, N.; Badawi, G.H.; Kaminaka, H.; Sanekata, T.; Shibahara, T.; Inanaga, S.; Tanaka, K. Overexpression of monodehydroascorbate reductase in transgenic tobacco confers enhanced tolerance to ozone, salt and polyethylene glycol stresses. *Planta* **2007**, *225*, 1255–1264. [\[CrossRef\]](#)
19. Stevens, R.; Page, D.; Gouble, B.; Garchery, C.; Zamir, D.; Causse, M. Tomato fruit ascorbic acid content is linked with monodehydroascorbate reductase activity and tolerance to chilling stress. *Plant Cell Environ.* **2008**, *31*, 1086–1096. [\[CrossRef\]](#)
20. Gill, S.S.; Tuteja, N. Reactive oxygen species and antioxidant machinery in abiotic stress tolerance in crop plants. *Plant Physiol. Biochem.* **2010**, *48*, 909–930. [\[CrossRef\]](#)
21. Park, A.K.; Kim, I.S.; Do, H.; Jeon, B.W.; Lee, C.W.; Roh, S.J.; Shin, S.C.; Park, H.; Kim, Y.S.; Kim, Y.H.; et al. Structure and catalytic mechanism of monodehydroascorbate reductase, MDHAR, from *Oryza sativa* L. japonica. *Sci. Rep.* **2016**, *6*, 33903. [\[CrossRef\]](#) [\[PubMed\]](#)
22. Parnikoza, I.Y.; Maidanuk, D.N.; Kozeretska, I.A. Are *Deschampsia antarctica* Desv. and *Colobanthus quitensis* (Kunth) Bartl. migratory relicts? *Tsitol. Genet.* **2007**, *41*, 36–40. [\[CrossRef\]](#) [\[PubMed\]](#)
23. Santiago, I.F.; Alves, T.M.; Rabello, A.; Sales, P.A., Jr.; Romanha, A.J.; Zani, C.L.; Rosa, C.A.; Rosa, L.H. Leishmanicidal and antitumoral activities of endophytic fungi associated with the Antarctic angiosperms *Deschampsia antarctica* Desv. and *Colobanthus quitensis* (Kunth) Bartl. *Extremophiles* **2012**, *16*, 95–103. [\[CrossRef\]](#) [\[PubMed\]](#)
24. Otwinowski, Z.; Minor, W. Processing of X-ray diffraction data collected in oscillation mode. *Method Enzymol.* **1997**, *276*, 307–326. [\[CrossRef\]](#)
25. Vagin, A.; Teplyakov, A. Molecular replacement with MOLREP. *Acta Cryst. D* **2010**, *66*, 22–25. [\[CrossRef\]](#) [\[PubMed\]](#)
26. Murshudov, G.N.; Skubak, P.; Lebedev, A.A.; Pannu, N.S.; Steiner, R.A.; Nicholls, R.A.; Winn, M.D.; Long, F.; Vagin, A.A. REFMAC5 for the refinement of macromolecular crystal structures. *Acta Cryst. D* **2011**, *67*, 355–367. [\[CrossRef\]](#)
27. Emsley, P.; Lohkamp, B.; Scott, W.G.; Cowtan, K. Features and development of Coot. *Acta Cryst. D* **2010**, *66*, 486–501. [\[CrossRef\]](#)
28. Chen, V.B.; Arendall, W.B.; Headd, J.J.; Keedy, D.A.; Immormino, R.M.; Kapral, G.J.; Murray, L.W.; Richardson, J.S.; Richardson, D.C. MolProbity: All-atom structure validation for macromolecular crystallography. *Acta Cryst. D* **2010**, *66*, 12–21. [\[CrossRef\]](#)
29. DeLano, W.L. *The PyMOL Molecular Graphics System*; Schrodinger: New York, NY, USA, 2010; Version 1.3r1; Available online: <http://pymol.sourceforge.net/overview/index.htm> (accessed on 18 September 2019).
30. Jeong, J.Y.; Yim, H.S.; Ryu, J.Y.; Lee, H.S.; Lee, J.H.; Seen, D.S.; Kang, S.G. One-step sequence- and ligation-independent cloning as a rapid and versatile cloning method for functional genomics studies. *Appl. Environ. Microbiol.* **2012**, *78*, 5440–5443. [\[CrossRef\]](#)
31. Gietz, R.D.; Schiestl, R.H. High-efficiency yeast transformation using the LiAc/SS carrier DNA/PEG method. *Nat. Protoc.* **2007**, *2*, 31–34. [\[CrossRef\]](#)
32. Senda, M.; Kishigami, S.; Kimura, S.; Fukuda, M.; Ishida, T.; Senda, T. Molecular mechanism of the redox-dependent interaction between NADH-dependent ferredoxin reductase and rieske-type [2Fe-2S] ferredoxin. *J. Mol. Biol.* **2007**, *373*, 382–400. [\[CrossRef\]](#) [\[PubMed\]](#)
33. Li, F.; Wu, Q.Y.; Sun, Y.L.; Wang, L.Y.; Yang, X.H.; Meng, Q.W. Overexpression of chloroplastic monodehydroascorbate reductase enhanced tolerance to temperature and methyl viologen-mediated oxidative stresses. *Physiol. Plant.* **2010**, *139*, 421–434. [\[CrossRef\]](#) [\[PubMed\]](#)
34. Sultana, S.; Khew, C.-Y.; Morshed, M.M.; Namasivayam, P.; Napis, S.; Ho, C.-L. Overexpression of monodehydroascorbate reductase from a mangrove plant (AeMDHAR) confers salt tolerance on rice. *J. Plant Physiol.* **2012**, *169*, 311–318. [\[CrossRef\]](#) [\[PubMed\]](#)

35. Liu, J.; Sun, X.; Xu, F.; Zhang, Y.; Zhang, Q.; Miao, R.; Zhang, J.; Liang, J.; Xu, W. Suppression of OsMDHAR4 enhances heat tolerance by mediating H₂O₂-induced stomatal closure in rice plants. *Rice* **2018**, *11*, 38. [[CrossRef](#)] [[PubMed](#)]
36. Yeh, H.-L.; Lin, T.-H.; Chen, C.-C.; Cheng, T.-X.; Chang, H.-Y.; Lee, T.-M.; Hsin-Yang, C. Monodehydroascorbate reductase plays a role in the tolerance of *Chlamydomonas reinhardtii* to photooxidative stress. *Plant Cell Physiol.* **2019**, *60*, 2167–2179. [[CrossRef](#)]



© 2019 by the authors. Licensee MDPI, Basel, Switzerland. This article is an open access article distributed under the terms and conditions of the Creative Commons Attribution (CC BY) license (<http://creativecommons.org/licenses/by/4.0/>).